Geophysical Research Letters

RESEARCH LETTER
10.1029/2022GL097899

The Role of Atmospheric Blocking in Regulating Arctic Warming

Cheng You[1], Michael Tjernström[1], Abhay Devasthale[2], and Daniel Steinfeld[3]

[1]Department of Meteorology & Bolin Centre for Climate Research, Stockholm University, Stockholm, Sweden, [2]Remote Sensing Unit, Research and Development Department, Swedish Meteorological and Hydrological Institute, Norrköping, Sweden, [3]Institute of Geography and Oeschger Centre for Climate Change Research, University of Bern, Bern, Switzerland

Key Points:

- The more frequently occurring blocking anticyclones contribute to the increasing poleward energy transport during last 40 year
- In winter, this increasing poleward energy transport leads to regional warming trend over the Barents Sea
- In summer, regional warming trend is dominated by the subsidence and solar radiation inside the more frequently occurring blocks

Supporting Information:

Supporting Information may be found in the online version of this article.

Correspondence to:

C. You,
cyoupuguan@gmail.com

Citation:

You, C., Tjernström, M., Devasthale, A., & Steinfeld, D. (2022). The role of atmospheric blocking in regulating Arctic warming. *Geophysical Research Letters*, *49*, e2022GL097899. https://doi.org/10.1029/2022GL097899

Received 23 JAN 2022
Accepted 31 MAY 2022

Author Contributions:

Conceptualization: Michael Tjernström
Funding acquisition: Michael Tjernström, Abhay Devasthale
Methodology: Daniel Steinfeld
Project Administration: Michael Tjernström, Abhay Devasthale
Supervision: Michael Tjernström, Abhay Devasthale
Writing – review & editing: Michael Tjernström, Abhay Devasthale, Daniel Steinfeld

Abstract Using ERA5 reanalysis we find positive trends in poleward transport of moisture and heat during 1979–2018 over the winter Barents Sea sector and summer East Siberian Sea sector. The increase in blocking occurrence (blocking days) can explain these trends. Blocking occurrence over the Barents Sea sector significantly increased in the last 40 winters, inducing increasingly stronger poleward transport of moisture and heat. The high linear correlation between poleward energy transports and temperature over the Barents Sea sector suggests that poleward energy transports dominate the regional warming trend there. Meanwhile, in summer, more frequently occurring blocking over the Beaufort Sea sector causes a positive trend of poleward moist and heat transport over the East Siberian Sea sector. The high linear correlation between the blocking occurrence and temperature suggests that the increasing shortwave radiation and subsidence within the more frequently occurring blocking contribute to the regional warming trend.

Plain Language Summary During last 40 year, Anticyclones become more frequent over the Arctic. To the west of these more frequently occurring Anticyclones, warm and moist air are transported into the Arctic region more frequently. In winter, these more frequent transports of moisture and heat into the Arctic lead to the amplified regional warming trend over the Barents Sea. However, these transports do not contribute significantly to the summer regional warming trend. Instead, the amplified summer regional warming always occurs over the region with more frequently occurring anticyclones, suggesting that the increasing solar radiation and subsidence within the more frequently occurring anticyclones lead to the summer regional warming trend.

1. Introduction

The near-surface warming in the Arctic is more than twice as fast as the global mean warming in recent decades. This phenomenon, known as Arctic amplification, is a key aspect of climate change (Cohen et al., 2014; Serreze et al., 2006, 2009, 2012). However, its exact mechanism is still under debate. A wide range of local and remote processes are considered modulators to Arctic Amplification. Examples of local processes are albedo feedback (Pithan & Mauritsen, 2014; Screen & Simmonds, 2010b), water vapor content (Serreze et al., 2012), air-sea heat exchange (Boisvert et al., 2016; Kim et al., 2019; Screen & Simmonds, 2010a; Sotiropoulou et al., 2016) and downwelling longwave irradiance induced by clouds (Kapsch et al., 2013). Remote processes like oceanic and atmospheric poleward transport of heat and moisture (Årthun & Eldevik, 2016; Naakka et al., 2019; Tjernström et al., 2015a; Woods & Caballero, 2016) could also be partially responsible for the Arctic Amplification. Especially, over winter Barents Sea, poleward moisture transport (hereafter PMT) can statistically explain a substantial part of the winter surface warming and sea ice melting (Woods & Caballero, 2016). Intensive PMT over all sectors of the Arctic Ocean typically feature a block to the east and a low-pressure to the west, implying that intensive PMT is driven by blocks (Binder et al., 2017; Fearon et al., 2021; Messori et al., 2018; Papritz, 2020; You et al., 2021a, 2021b).

The mechanism behind the formation and maintenance of such Arctic blocks is still unclear. A positive North Atlantic Oscillation (NAO) favors the development of Arctic blocks over the Barents Sea through Rossby wave train propagation (Luo et al., 2016). Recently, cloud-diabatic processes in the ascending warm conveyor belt of extratropical cyclones have been found to contribute substantially to establishing Arctic blocks. These warm conveyor belts transport air masses with low potential vorticity cross-isentropically from the lower troposphere

into the upper troposphere (Pfahl et al., 2015; Steinfeld & Pfahl, 2019; Svensson & Karlsson, 2011; Wernli & Papritz, 2018).

There are many blocking detection algorithms available in the literature, such as the TM index (Tibaldi & Molteni, 1990), the pv-θ index (Tyrlis et al., 2015, 2019, 2020), and the Absolute Geopotential Height reversal method (AGH; Davini et al., 2012). The TM index has been utilized to identify Ural blocking, believed to contribute to the accelerated sea ice loss over the Barents Sea (Gong & Luo, 2017; Luo et al., 2016). This index requires a positive meridional height gradient and a significant westerly flow within the 40°–60°N and the 60°–80°N latitude bands, respectively. For a blocking detection with TM index, defining a longitude band is also necessary, which brings spatial limitation for Arctic blocking detection. Tyrlis et al. (2021) studied high-latitude blocks with both the pv-θ and the AGH indexes and showed that although they agree on the detection of midlatitude blocks, they have a large discrepancy in the frequency of the high-latitude blocks. To avoid the problems brought by above-mentioned blocking detection methods, the blocking track algorithm based on potential vorticity (Schwierz et al., 2004) is used here. This algorithm tracks and quantifies all blocks globally and works well also over the high Arctic (Wernli & Papritz, 2018). It follows the entire life cycle of blocks, quantifying their intensity, occurrence and persistence. Using this blocking track algorithm, we attempt to study if the amplified Arctic warming is attributable to the increasing Arctic blocking occurrence.

2. Methods

As atmospheric blocks occur, a negative potential vorticity anomaly (APV) is always located in the immediate vicinity of the tropopause. Therefore, a major negative APV is one indicator of a strong anticyclonic circulation, providing the dynamical basis for the blocking track algorithm used here (Schwierz et al., 2004; Sprenger et al., 2017). In this algorithm, the vertically averaged APV between 500 and 150 hPa is used as the indicator of blocks, defined as the closed contour of APV at the value of −1.3 PVU (1 PVU equals to 10^{-6} m^2 s^{-1}K kg^{-1}). In other words, the areas with negative APV which is not larger than −1.3 PVU are considered blocks. More negative APV indicates stronger blocks. If the block at nearby time steps overlaps more than 70%, then it is assumed to belong to the same blocking life-cycle (Figure S1a in Supporting Information S1). Here, we only consider blocks with a life-time of at least 5 days. The increase/decrease of blocking life-time can decrease/increase the magnitude of blocking frequency but does not change its geographical distribution. This blocking track algorithm is applied to the European Center for Medium-Range Weather Forecast latest reanalysis, ERA5 (Hersbach et al., 2020), with a 6-hourly temporal resolution and a 0.75° horizontal resolution. We explore all blocking life-cycles from 1979 to 2018, using a 1-day running average before applying the blocking track algorithm.

Considering the winter (DJF) and summer (JJA) seasons separately, a record of the locations of each identified blocking is kept throughout its life cycle. Figure S1a in Supporting Information S1 shows schematic examples of the 6-hourly footprints of two individual blocks. The occurrence and the number of individual blocks are accumulated at each grid point; occurrence is defined as the total number of blocking days at each grid point. For instance, in Figure S1a in Supporting Information S1, the blocking occurrence at grid points A, B, and C are 1.25, 2, and 1.75 days, respectively, as the paths of the two blocks partially overlap. Blocking number is defined as the number of individual blocks that pass over each grid point. Hence, in Figure S1b in Supporting Information S1, the blocking number at grid points D, E, F, and G are 3, 4, 2, and 1, respectively. The averaged APV at each point when blocking occurs is considered blocking intensity, while the accumulated blocking occurrence divided by accumulated blocking number is considered the mean blocking persistence.

Monthly mean poleward moisture (PMT) and heat transport (PHT) are evaluated in the ERA5 reanalysis data set by the vertical integral of northward water vapor and heat fluxes from the surface of the Earth to the top of the atmosphere, respectively, as shown by following equations:

$$\mathrm{PMI} = -\frac{1}{g}\int_{sfc}^{top} v\,q\,\mathrm{d}p \tag{1a}$$

$$\mathrm{PHT} = -\frac{1}{g}\int_{sfc}^{top} v\,T\,\mathrm{d}p \tag{1b}$$

where v is northward velocity, T is air temperature, q is specific humidity and g is gravitational acceleration. Besides, all other variables used in this paper, such as temperature, geopotential height, and surface energy-budget terms are derived from ERA5 reanalysis data set.

3. Results

3.1. Winter Poleward Moisture and Heat Transport

We identify positive trends of PMT and PHT during recent 40 winters over the Barents Sea sector, at 3 kg m^{-1} s^{-1} $decade^{-1}$ and 1.2×10^8 W m^{-1} $decade^{-1}$, respectively, while a negative trend of PMT is located over the western Siberia (Figure 1a). Similar monthly trends of PMT have also been found by Rinke et al. (2019). South of 85°N, a positive trend of PHT is located slightly to the west of its PMT counterpart, but they overlap north of 85°N (Figure 1). All trends are significant at the 95% level and we consider the region with a significant positive PMT trend a sensitive region (highlighted by green dots at Figure 1a). No significant trend of zonal moisture or heat transport was found over this sensitive region. The mean sea ice concentration (SIC), temperature at 850 hPa (T_{850}), PHT and PMT in the sensitive region have large interannual variations (Figure 2b) but display significant linear trends (Figure S2a in Supporting Information S1). Mean T_{850}, PHT and PMT have positive trends, while SIC has negative trend (Figure S2a in Supporting Information S1). Not surprisingly, temperature has high linear correlation with PHT and PMT; 0.78 and 0.85 respectively. Linear regression indicates that positive PMT is correlated to the blocking over the Barents-Kara Sea sector (Figure S3a in Supporting Information S1). As this blocking occurs, warm and moist Atlantic air is transported into the high Arctic (positive T_{advct} in Figure S3d in Supporting Information S1), leading to a positive temperature anomaly over the Barents Sea sector (Figure S3c in Supporting Information S1), also exerting positive anomalies of turbulent heat and longwave radiation fluxes at the surface (Figure S4 in Supporting Information S1). Consequently, it contributes to sea ice decrease over the Barents Sea sector (Figure S3b in Supporting Information S1). Many previous studies have reached similar conclusions (Binder et al., 2017; Gong & Luo, 2017; Kim et al., 2019; Luo et al., 2016; Sedlar et al., 2011), but few elaborate on the cause of this positive PMT trend over the Barents Sea sector.

Since the blocking can statistically explain the positive anomalies of PMT and PHT over the Barents Sea sector, we further explore if trends in blocking occurrence can also explain the positive trends of PMT and PHT. The trend of 2D moisture/heat transport (vector field in Figures 1a and 1b) suggests a positive trend of anti-cyclonic circulation over the Barents Sea sector, to some extent, supporting this hypothesis. To test this hypothesis, we quantify Arctic blocking occurrence with the method described in Section 2. During the last 40 winters, blocking occurrence has increased at a rate of ~3 days $decade^{-1}$ (Figure 1c) at exactly the location where the positive GH anomaly is located (Figure S3a in Supporting Information S1). Meanwhile, in the vicinity of these more frequently occurring blocks, T_{850} has increased by > 1 K $decade^{-1}$ (Figure 1e), while SIC decreases by > 20% $decade^{-1}$ (Figure 1d). The spatial structure of the trends in SIC, T_{850}, temperature advection (T_{advct}) in Figure 1 are all similar to their corresponding anomalies based on regression in Figure S3 in Supporting Information S1, further supporting the hypothesis.

To further understand the cause of the increased blocking occurrence, we quantify if this positive trend comes from the increase in blocking number or blocking persistence. As shown in Figures 2a and 2b significant positive trend in blocking persistence is found exactly in the region where positive trend of blocking occurrence occurs, which implies that the increasing blocking occurrence is due to longer blocking durations, rather than to an increase in number of events. The blocking intensity is also significantly strengthened to the east of Svalbard in the last 40 yr (Figure 2c). Even though positive trend in blocking number also occurs near the northwestern Scandinavian coast, and the eastern and northeastern coast of Greenland (Figure 2a), this does not contribute to any significant positive trend of blocking occurrence over the Barents Sea sector.

The anticyclonic flow around the blocks leads to equatorward flow to the east of the block. As the blocks occur more frequently over the Barents Sea sector, a negative trend of PMT, PHT (not significant) and temperature advection are found to the east of the blocks, indicating more frequent cold air outbreak over Siberia (Figures 1a and 1b). In conjunction with more positive PMT and PHT events occurring over the Barents Sea sector, the climate pattern of warm Barents and cold Siberia has become more frequent during past 40 yr.

10.1029/2022GL097899

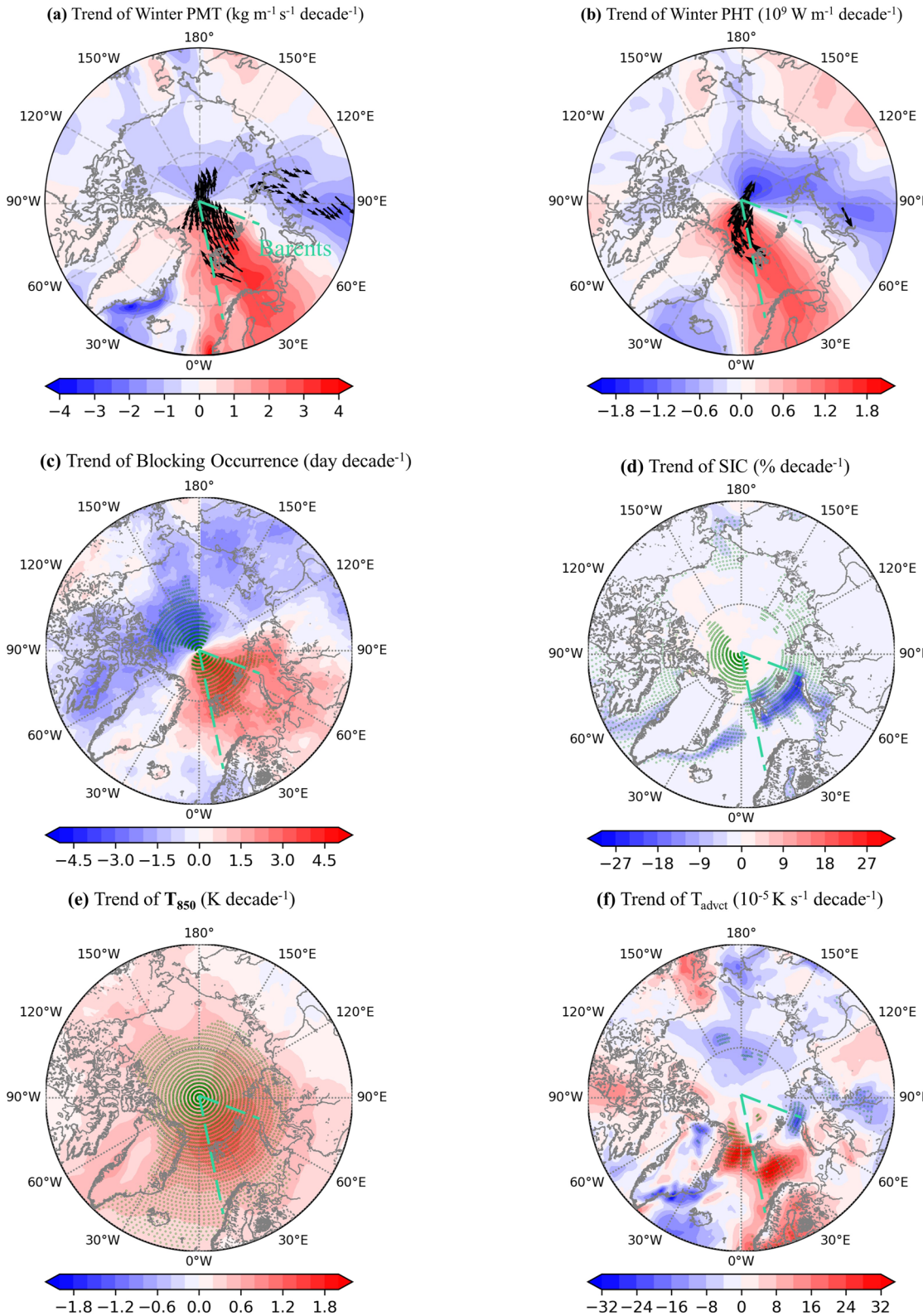

Figure 1. The linear trend of (a) poleward moisture transport (PMT) and 2D moisture transport (vectors), (b) poleward heat transport (PHT) and 2D heat transport (vectors), (c) blocking occurrence, (d) sea ice concentration (SIC), (e) 850 hPa temperature (T_{850}), and (f) temperature advection (T_{advct}) during 1979–2018 winter. The stippling including vectors in Figures 1a and 1b indicates statistical significance at the $p < 0.05$ level from a Student's t test. The westmost and eastmost limit of Barents Sea sector is highlighted by cyan dash lines.

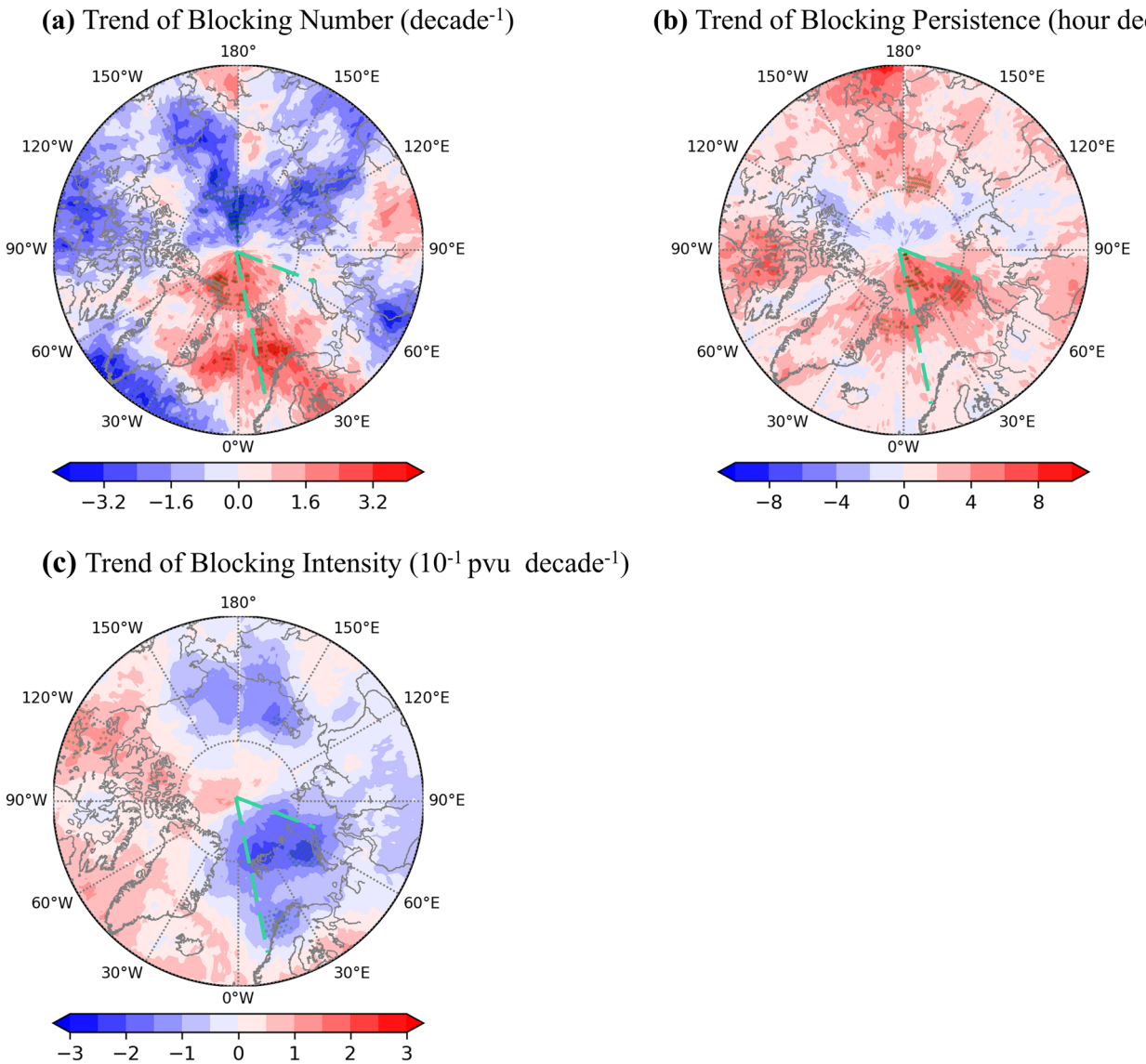

Figure 2. The linear trend of (a) blocking number, (b) blocking persistence and (c) blocking intensity during 1979–2018 winter. The stippling indicates statistical significance at the $p < 0.1$ level from a Student's t test. The westmost and eastmost limit of Barents Sea sector is highlighted by cyan dash lines. Note that negative trend in blocking intensity means intensified blocks since the absolute value of the blocking intensity is negative by definition.

3.2. Summer Poleward Moisture and Heat Transport

In summer, significant positive trends in both PMT and PHT are found over the East Siberian Sea sector, with significant negative trends over the Barents Sea sector (Figure 3). We take the region with significant positive PMT trend as a sensitive region. Similar to the winter PMT/PHT over the Barents Sea sector, the positive mean PMT and PHT in the sensitive region can also be statistically explained by an Arctic blocking (Figure S5a in Supporting Information S1). This Arctic blocking transports warm and moist air from lower latitudes into the Arctic, inducing warming anomalies (Figure S5c in Supporting Information S1) and sea ice melt (Figure S5b in Supporting Information S1), presumably due to positive anomalies in longwave radiation (Figure S4b in Supporting Information S1) and turbulent heat flux (Figures S6d and S6e in Supporting Information S1), despite negative shortwave radiation anomalies (Figure S6c in Supporting Information S1). Similar results are also shown by Tjernström et al. (2015b) and You et al. (2020, 2021a). However, unlike its winter counterpart where the positive temperature anomaly is located between positive and negative GH anomalies (Figures S3a and S3c in Supporting Information S1), the summer positive temperature anomaly is located almost entirely in the area with

10.1029/2022GL097899

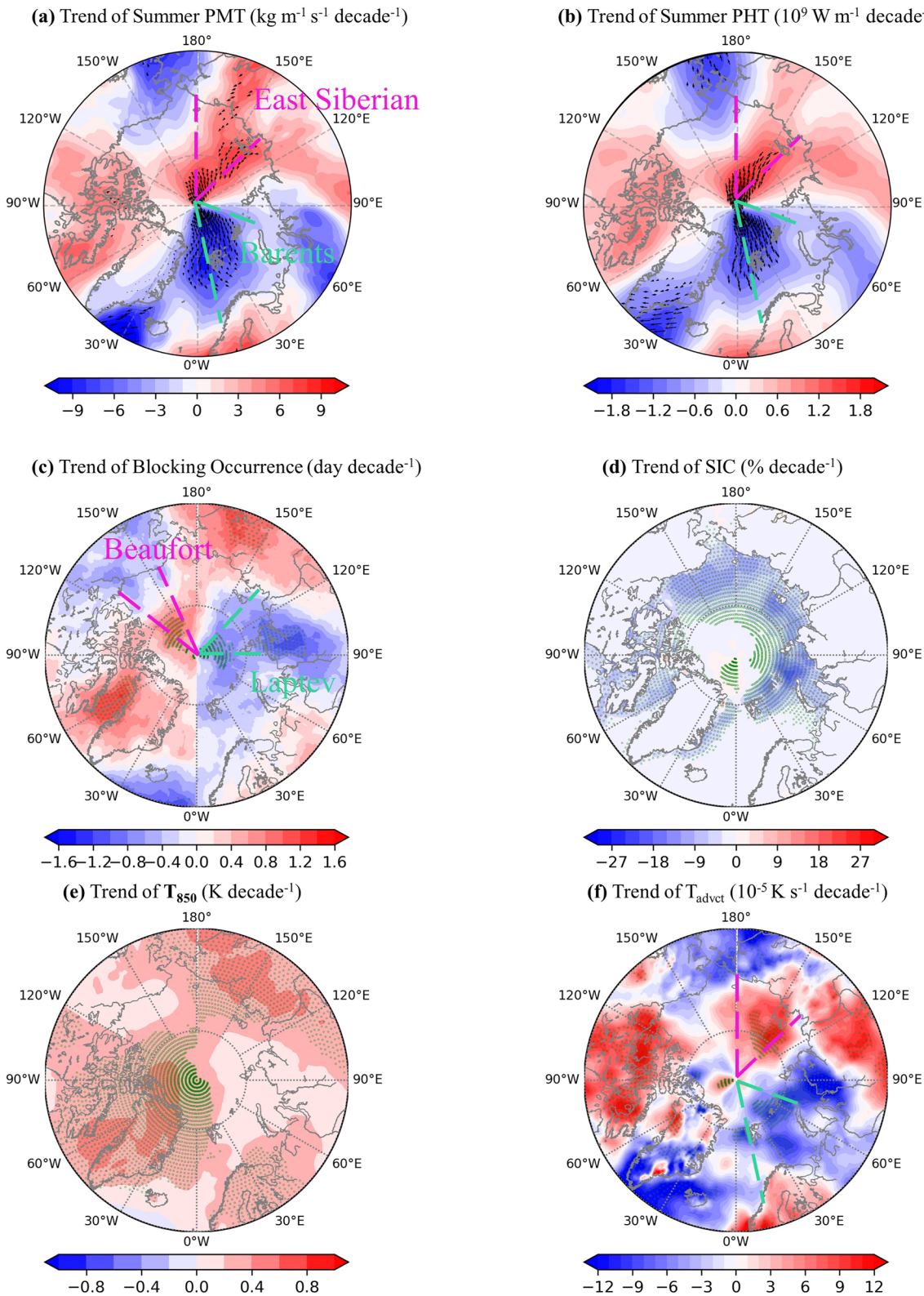

Figure 3. The linear trend of (a) poleward moisture transport (PMT) and 2D moisture transport (vectors), (b) poleward heat transport (PHT) and 2D heat transport (vectors), (c) blocking occurrence, (d) sea ice concentration (SIC), (e) 850 hPa temperature (T_{850}), and (f) temperature advection (T_{advct}) during 1979–2018 summer (JJA). The stippling including vectors in Figures 3a and 3b indicates statistical significance at the $p < 0.05$ level from a Student's t test. The westmost and eastmost limit of Sea sectors are highlighted by cyan or magenta dash lines.

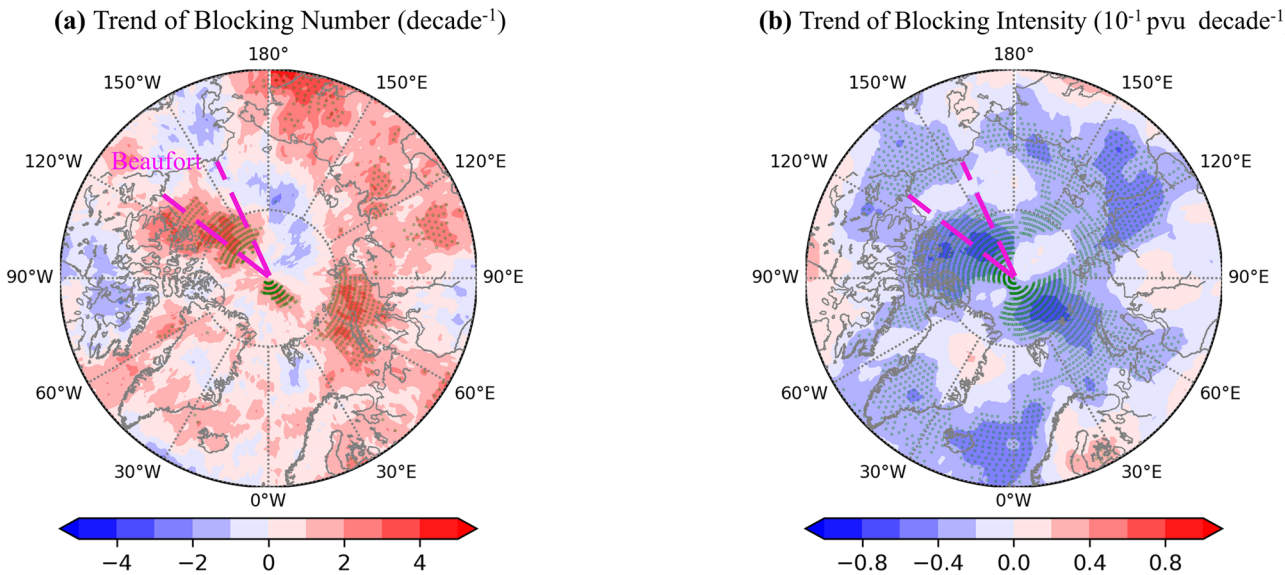

Figure 4. The linear trend of (a) blocking number, (b) blocking intensity during 1979–2018 summer. The stippling indicates statistical significance at the $p < 0.1$ level from a Student's t test. The westmost and eastmost limit of Beaufort Sea sector is highlighted by magenta dash lines.

positive GH anomaly (Figure S5b in Supporting Information S1), while the net surface energy-budget is greatly enhanced within the anticyclonic anomaly and not in the area with warm advection (Figure S6a in Supporting Information S1). Although T_{850} is positively correlated with PMT and PHT (correlation coefficients 0.39 and 0.45, respectively), the correlation is weaker than that in winter (Figure S7 in Supporting Information S1). This implies that, in summer, subsidence and solar irradiance in blocks (Figure S6c in Supporting Information S1) are more important to the local warming than the poleward energy transport, in agreement with Kay et al. (2008) and Papritz (2020). The preliminary results show that the regional warming over the Baffin Bay is dominated by increased solar irradiance, while the regional warming over the Beaufort Sea sector is dominated by the enhanced subsidence. The exact contribution from subsidence and net solar irradiance will be quantified in the future case studies.

The positive trends in PMT and PHT during summer can also be statistically explained by increasing blocking occurrence (Figure 3c). Blocking occurrence is increasing by ∼1 day decade^{-1} over the Beaufort Sea sector. It is decreasing over the East Siberian Sea sector (∼ −0.8 days decade^{-1}), probably suggesting that low-pressure systems (cyclones) are occurring more often over the East Siberian Sea sector (Akperov et al., 2019). Between the cyclone and blocking exist great geopotential height gradient which induces strong poleward moist and heat transport. As both of the cyclone and blocking occur more frequently, both PMT and PHT have positive trends between these two more prevailing systems; 7 kg m^{-1} s^{-1} decade^{-1} and 1.2×10^8 W m^{-1} decade^{-1}, respectively. This hypothesis is also supported by the similarity in T_{advct} between Figure 3f and Figure S5d in Supporting Information S1, as well as the similarity in SIC between Figure 3d and Figure S5d in Supporting Information S1. The increasing blocking occurrence over the Beaufort Sea sector is mostly contributed by an increasing blocking number (∼4 decade^{-1}) while the intensity of blocks is also intensified in the last 40 yr (Figure 4).

The linear correlation coefficient of 0.74 between T_{850} and blocking occurrence over the Beaufort Sea sector is larger than that between T_{850} and PMT (0.39) in the sensitive region (Figure S8a in Supporting Information S1). T_{850} shares the same magnitude of linear trend as blocking occurrence in last 40 summers (Figure S8b in Supporting Information S1), which implies that in summer the blocks contribute more to the Arctic warming than the warm advection. This is the case not only over the Beaufort Sea sector; there is always a positive trend of blocking occurrence in the region with a positive trend in T_{850}. Over Baffin Bay for example (Figure S9 in Supporting Information S1), the linear correlation coefficient (0.85) is even higher than that over the Beaufort Sea sector.

4. Discussion

Low-pressure systems over the Iceland always cooperate with the blocking over the Barents Sea to transport moisture and heat into the high Arctic (Figure S3a in Supporting Information S1). As we trace the development of the blocking over the Barents Sea sector, it is found that it often originates from a low-pressure system near Iceland about 6 days before the PMT peak (Figure S10 in Supporting Information S1). After 6 days as the PMT reaches the maximum, the positive NAO develops into a Rossby wave train (Figure S10 in Supporting Information S1), as also discussed by Luo et al. (2016). Low-pressure systems have been found to contribute substantially to establish Arctic blocks by transporting low PV air cross-isentropically from the lower troposphere into the upper troposphere (Murto et al., 2022; Steinfeld & Pfahl, 2019; Wernli & Papritz, 2018). Therefore, we hypothesize that more predominant low-pressure systems lead to the increasing blocking occurrence. We attempted to quantify the occurrence of the low-pressure systems with similar methodology as the blocking detection algorithm, but find no significant trend over the Iceland in winter.

Due to the amplified Arctic warming, the poleward temperature gradient decreases at high-latitude region, weakening the westerly winds and therefore weather patterns like blocks may move eastward more slowly (Overland et al., 2015; Yao et al., 2017). This could explain that the increasing blocking persistence mainly contributes to the more frequently occurring blocks over the Barents Sea sector. Luo et al. (2017) carried out idealized numerical experiments under strong and weak mean flow to test this hypothesis. These more persistent blocks would pump more heat and moist into the Arctic, more intensively warming the Arctic and in turn further weakening the mean flow, as synthesized in Figure 5a. Some studies also argued that storms also contribute to the PMT transport (Rinke et al., 2017). However, without the poleward steering of blocks, transient moisture transport by a storm may not contribute much to the year-to-year trend of PMT/PHT during last 40 yr, as the positive PMT/PHT caused by the east side of the storm may offset the negative PMT/PHT induced at the west of the storm. The other point is that blocking as a larger scale pattern can continuously bring even warmer air mass into the high Arctic for days. In some cases when storm and blocking occur together, they can transport extremely more warm air mass into the Arctic (Binder et al., 2017; Murto et al., 2022).

In summer, the development of Beaufort blocking also statistically originates from the low-pressure system over the Bering Sea (Figure S11 in Supporting Information S1), in agreement with case studies in Wernli and Papritz (2018). Different from its winter counterpart, however, the more frequently occurring blocks over the summer Beaufort Sea sector result from the increased blocking number, which cannot be explained by weakened westerlies. Unlike the winter Barents Sea sector, the main causes of summer Arctic warming are the enhanced subsidence and surface solar irradiance in the more frequently occurring blocks. Since the ice albedo feedback only can explain ∼30% of surface Arctic warming in summer (Graversen & Wang, 2009), therefore contributors related to the blocks, such as solar irradiance, subsidence and solar radiations within the blocking anticyclones could be potentially responsible for the rest (70%) of Arctic warming, as synthesized in Figure 5b.

5. Conclusions

Using ERA5 reanalysis, the Arctic warming amplification is attributed to the increasing occurrence of Arctic blocking. According to previous studies, poleward moist and heat transport contribute to the Arctic warming. Positive PMT and heat transport is statistically related to blocks. In this research, a positive trend of PMT and heat transport during 1979–2018 is identified over the winter Barents Sea sector (3 kg m^{-1} s^{-1} $decade^{-1}$; 1.2×10^8 W m^{-1} $decade^{-1}$) and for the summer East Siberian Sea sector (7 kg m^{-1} s^{-1} $decade^{-1}$; 1.2×10^8 W m^{-1} $decade^{-1}$). We have attributed these positive trends to the increased blocking occurrence as quantified with a blocking tracking algorithm. Unlike other blocking detection methods, this algorithm captures Arctic blocks by tracking each blocking separately through its entire life cycles. Based on this algorithm, we evaluated the trend of blocking occurrence, blocking persistence, and blocking number at each grid point.

We find that Barents Sea blocks occur more often and are more intensive during last 40 winters, at the rates of ∼3 days $decade^{-1}$ and −0.25 PVU $decade^{-1}$, respectively, and induce increasingly stronger poleward moist/heat transport over the Barents Sea sector, leading to surface warming and sea ice melt. This increasing blocking occurrence is mainly due to longer blocking persistence (by ∼8 hr $decade^{-1}$). Meanwhile, more blocks over the Beaufort Sea sector (∼1 day $decade^{-1}$) cause a positive trend of poleward moist and heat transport over the East Siberian Sea sector (7 kg m^{-1} s^{-1} $decade^{-1}$ and 1.2×10^8 W m^{-1} $decade^{-1}$, respectively), inducing surface warming

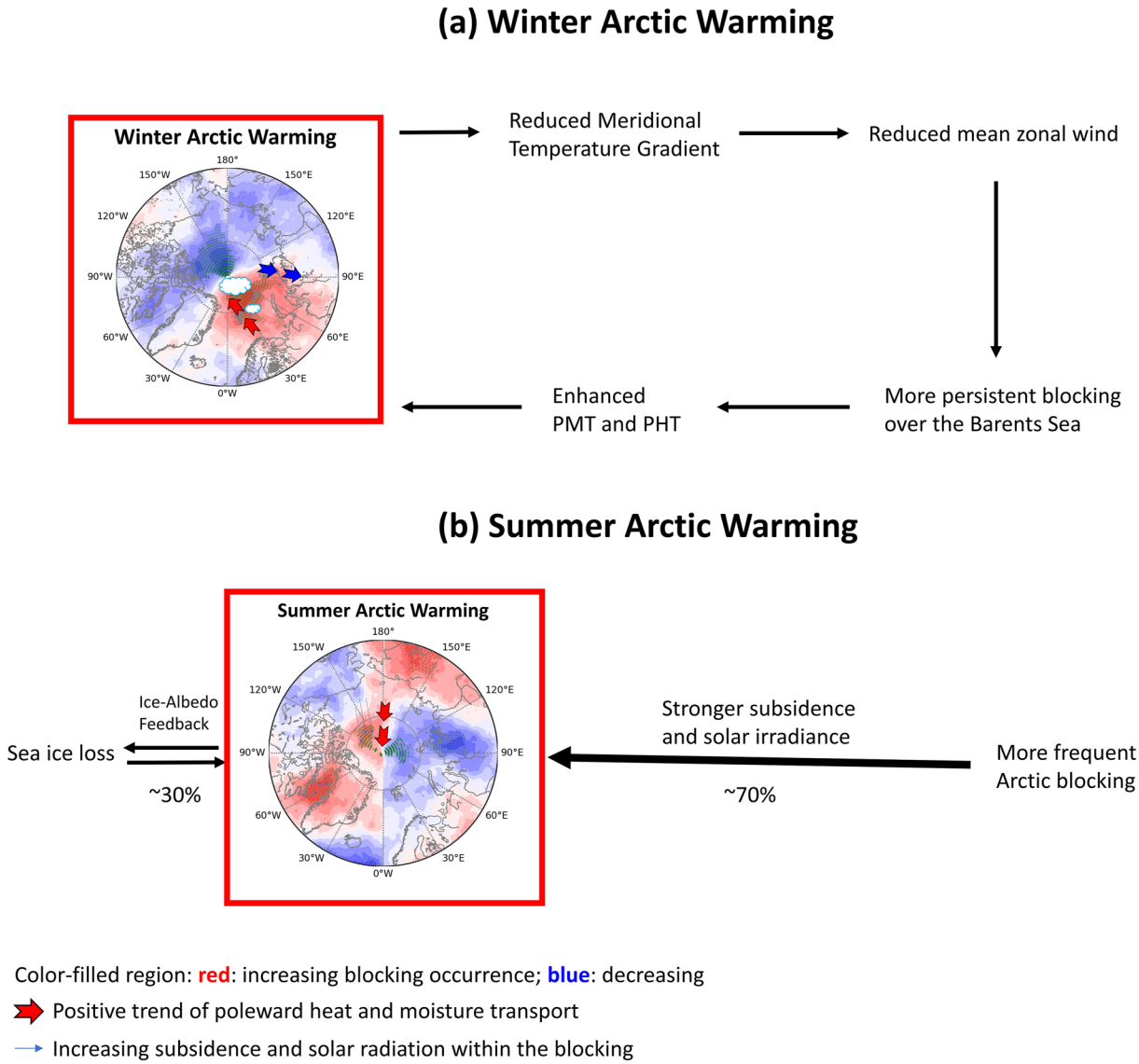

Figure 5. Conceptual figure for winter (a) and summer (b) Arctic warming mechanisms.

and sea ice melt. However, in summer, enhanced solar irradiance and subsidence within the more frequently occurring blocks contribute more to the surface warming than the warm advection that occurs to the west of blocks. Over the Beaufort Sea sector, the blocking occurrence has large linear correlation with temperature during last 40 summers. The increased summer blocking occurrence is mainly contributed by the increased blocking numbers (~4 decade^{-1}). Other regions, like Baffin Bay and Far East Russia, also display a larger occurrence of blocks, with corresponding temperature increase. However, the potential reason of the increased summer Arctic blocking number is still unclear and deserves more attentions from atmospheric scientists.

Data Availability Statement

All data used can be found on the ERA5 reanalysis data set (Hersbach et al., 2020) at DOI: https://doi.org/10.24381/cds.f17050d7. Figures were made with Matplotlib version 3.1.3 (Caswell et al., 2020; Hunter, 2007), available under the Matplotlib license at https://matplotlib.org/.The blocking identification code CONTRACK (Schwierz et al., 2004) is available at https://doi.org/10.5281/ZENODO.4765560 (Steinfeld, 2021).

Acknowledgments
This work was funded by the Swedish Research Council under Grant 2016-03807. The authors are grateful to Sonja Murto for helpful discussions on blocking formation in the Arctic.

References

Akperov, M., Rinke, A., Mokhov, I. I., Semenov, V. A., Parfenova, M. R., Matthes, H., et al. (2019). Future projections of cyclone activity in the Arctic for the 21st century from regional climate models (Arctic-CORDEX). *Global and Planetary Change*, *182*, 103005. https://doi.org/10.1016/j.gloplacha.2019.103005

Årthun, M., & Eldevik, T. (2016). On anomalous ocean heat transport toward the Arctic and associated climate predictability. *Journal of Climate*, *29*(2), 689–704. https://doi.org/10.1175/JCLI-D-15-0448.1

Binder, H., Boettcher, M., Grams, C. M., Joos, H., Pfahl, S., & Wernli, H. (2017). Exceptional air mass transport and dynamical drivers of an extreme wintertime Arctic warm event. *Geophysical Research Letters*, *44*(23), 12028–12036. https://doi.org/10.1002/2017GL075841

Boisvert, L. N., Petty, A. A., & Stroeve, J. C. (2016). The impact of the extreme winter 2015/2016 Arctic cyclone on the Barents-Kara Seas. *Monthly Weather Review*, *144*(11), 4279–4287. https://doi.org/10.1175/MWR-D-16-0234.1

Caswell, T. A., Droettboom, M., Lee, A., Hunter, J., Firing, E., Stansby, D., et al. (2020). *matplotlib/matplotlib v3.1.3*. https://doi.org/10.5281/ZENODO.3633844

Cohen, J., Screen, J. A., Furtado, J. C., Barlow, M., Whittleston, D., Coumou, D., et al. (2014). Recent Arctic amplification and extreme mid-latitude weather. *Nature Geoscience*, *7*, 627–637. https://doi.org/10.1038/ngeo2234

Davini, P., Cagnazzo, C., Gualdi, S., & Navarra, A. (2012). Bidimensional diagnostics, variability, and trends of Northern Hemisphere blocking. *Journal of Climate*, *25*(19), 6496–6509. https://doi.org/10.1175/JCLI-D-12-00032.1

Fearon, M. G., Doyle, J. D., Ryglicki, D. R., Finocchio, P. M., & Sprenger, M. (2021). The role of cyclones in moisture transport into the Arctic. *Geophysical Research Letters*, *48*, e2020GL090353. https://doi.org/10.1029/2020GL090353

Gong, T., & Luo, D. (2017). Ural blocking as an amplifier of the Arctic sea ice decline in winter. *Journal of Climate*, *30*(7), 2639–2654. https://doi.org/10.1175/JCLI-D-16-0548.1

Graversen, R. G., & Wang, M. (2009). Polar amplification in a coupled climate model with locked albedo. *Climate Dynamics*, *33*(5), 629–643. https://doi.org/10.1007/s00382-009-0535-6

Hersbach, H., Bell, B., Berrisford, P., Hirahara, S., Horányi, A., Muñoz-Sabater, J., et al. (2020). The ERA5 global reanalysis. *Quarterly Journal of the Royal Meteorological Society*, *146*(730), 1999–2049. https://doi.org/10.1002/qj.3803

Hunter, J. D. (2007). Matplotlib: A 2D graphics environment. *Computing in Science & Engineering*, *9*(3), 90–95. https://doi.org/10.1109/MCSE.2007.55

Kapsch, M. L., Graversen, R. G., & Tjernström, M. (2013). Springtime atmospheric energy transport and the control of Arctic summer sea ice extent. *Nature Climate Change*, *3*(8), 744–748. https://doi.org/10.1038/nclimate1884

Kay, J. E., L'Ecuyer, T., Gettelman, A., Stephens, G., & O'Dell, C. (2008). The contribution of cloud and radiation anomalies to the 2007 Arctic sea ice extent minimum. *Geophysical Research Letters*, *35*(8), L08503. https://doi.org/10.1029/2008GL033451

Kim, K. Y., Kim, J. Y., Kim, J., Yeo, S., Na, H., Hamlington, B. D., & Leben, R. R. (2019). Vertical feedback mechanism of winter Arctic amplification and sea ice loss. *Scientific Reports*, *9*, 1184. https://doi.org/10.1038/s41598-018-38109-x

Luo, D., Xiao, Y., Diao, Y., Dai, A., Franzke, C. L. E., & Simmonds, I. (2016). Impact of ural blocking on winter warm Arctic-cold Eurasian anomalies. Part II: The link to the North Atlantic Oscillation. *Journal of Climate*, *29*(11), 3949–3971. https://doi.org/10.1175/JCLI-D-15-0612.1

Luo, D., Yao, Y., Dai, A., Simmonds, I., & Zhong, L. (2017). Increased quasi stationarity and persistence of winter ural blocking and Eurasian extreme cold events in response to arctic warming. Part II: A theoretical explanation. *Journal of Climate*, *30*(10), 3569–3587. https://doi.org/10.1175/JCLI-D-16-0262.1

Messori, G., Woods, C., & Caballero, R. (2018). On the drivers of wintertime temperature extremes in the high Arctic. *Journal of Climate*, *31*(4), 1597–1618. https://doi.org/10.1175/JCLI-D-17-0386.1

Murto, S., Caballero, R., Svensson, G., & Papritz, L. (2022). Interaction between Atlantic cyclones and Eurasian atmospheric blocking drives wintertime warm extremes in the high Arctic. *Weather and Climate Dynamics*, *3*(1), 21–44. https://doi.org/10.5194/wcd-3-21-2022

Naakka, T., Nygård, T., Tjernström, M., Vihma, T., Pirazzini, R., & Brooks, I. M. (2019). The impact of radiosounding observations on numerical weather prediction analyses in the Arctic. *Geophysical Research Letters*, *46*(14), 8527–8535. https://doi.org/10.1029/2019GL083332

Overland, J., Francis, J. A., Hall, R., Hanna, E., Kim, S. J., & Vihma, T. (2015). The melting Arctic and midlatitude weather patterns: Are they connected? *Journal of Climate*, *28*(20), 7917–7932. https://doi.org/10.1175/JCLI-D-14-00822.1

Papritz, L. (2020). Arctic lower-tropospheric warm and cold extremes: Horizontal and vertical transport, diabatic processes, and linkage to synoptic circulation features. *Journal of Climate*, *33*(3), 993–1016. https://doi.org/10.1175/JCLI-D-19-0638.1

Pfahl, S., Schwierz, C., Croci-Maspoli, M., Grams, C. M., & Wernli, H. (2015). Importance of latent heat release in ascending air streams for atmospheric blocking. *Nature Geoscience*, *8*, 610–614. https://doi.org/10.1038/ngeo2487

Pithan, F., & Mauritsen, T. (2014). Arctic amplification dominated by temperature feedbacks in contemporary climate models. *Nature Geoscience*, *7*(3), 181–184. https://doi.org/10.1038/ngeo2071

Rinke, A., Maturilli, M., Graham, R. M., Matthes, H., Handorf, D., Cohen, L., et al. (2017). Extreme cyclone events in the Arctic: Wintertime variability and trends. *Environmental Research Letters*, *12*(9), 094006. https://doi.org/10.1088/1748-9326/aa7def

Rinke, A., Segger, B., Crewell, S., Maturilli, M., Naakka, T., Nygård, T., et al. (2019). Trends of vertically integrated water vapor over the Arctic during 1979–2016: Consistent moistening all over? *Journal of Climate*, *32*(18), 6097–6116. https://doi.org/10.1175/JCLI-D-19-0092.1

Schwierz, C., Croci-Maspoli, M., & Davies, H. C. (2004). Perspicacious indicators of atmospheric blocking. *Geophysical Research Letters*, *31*(6). https://doi.org/10.1029/2003gl019341

Screen, J. A., & Simmonds, I. (2010a). Increasing fall-winter energy loss from the Arctic Ocean and its role in Arctic temperature amplification. *Geophysical Research Letters*, *37*(16). L16707. https://doi.org/10.1029/2010GL044136

Screen, J. A., & Simmonds, I. (2010b). The central role of diminishing sea ice in recent Arctic temperature amplification. *Nature*, *464*(7293), 1334–1337. https://doi.org/10.1038/nature09051

Sedlar, J., Tjernström, M., Mauritsen, T., Shupe, M. D., Brooks, I. M., Persson, P. O. G., et al. (2011). A transitioning Arctic surface energy budget: The impacts of solar zenith angle, surface albedo and cloud radiative forcing. *Climate Dynamics*, *37*(7–8), 1643–1660. https://doi.org/10.1007/s00382-010-0937-5

Serreze, M. C., Barrett, A. P., & Stroeve, J. (2012). Recent changes in tropospheric water vapor over the Arctic as assessed from radiosondes and atmospheric reanalyses. *Journal of Geophysical Research*, *117*(10), D10104. https://doi.org/10.1029/2011JD017421

Serreze, M. C., Barrett, A. P., Stroeve, J. C., Kindig, D. N., & Holland, M. M. (2009). The emergence of surface-based Arctic amplification. *The Cryosphere*, *3*(1), 11–19. https://doi.org/10.5194/tc-3-11-2009

Serreze, M. C., & Francis, J. A. (2006). The Arctic amplification debate. *Climatic Change*, *76*(3–4), 241–264. https://doi.org/10.1007/s10584-005-9017-y

Sotiropoulou, G., Sedlar, J., Forbes, R., & Tjernström, M. (2016). Summer Arctic clouds in the ECMWF forecast model: An evaluation of cloud parametrization schemes. *Quarterly Journal of the Royal Meteorological Society*, *142*(694), 387–400. https://doi.org/10.1002/qj.2658

Sprenger, M., Fragkoulidis, G., Binder, H., Croci-Maspoli, M., Graf, P., Grams, C. M., et al. (2017). Global climatologies of Eulerian and Lagrangian flow features based on ERA-Interim. *Bulletin of the American Meteorological Society*, *98*(8), 1739–1748. https://doi.org/10.1175/BAMS-D-15-00299.1

Steinfeld, D. (2021). *steidani/ConTrack: ConTrack v0.3.0*. https://doi.org/10.5281/ZENODO.4765560

Steinfeld, D., & Pfahl, S. (2019). The role of latent heating in atmospheric blocking dynamics: A global climatology. *Climate Dynamics*, *53*(9–10), 6159–6180. https://doi.org/10.1007/s00382-019-04919-6

Svensson, G., & Karlsson, J. (2011). On the Arctic wintertime climate in global climate models. *Journal of Climate*, *24*(22), 5757–5771. https://doi.org/10.1175/2011JCLI4012.1

Tibaldi, S., & Molteni, F. (1990). On the operational predictability of blocking. *Tellus A: Dynamic Meteorology and Oceanography*, *42*(3), 343–365. https://doi.org/10.1034/j.1600-0870.1990.t01-2-00003.x

Tjernström, M., Shupe, M. D., Brooks, I. M., Persson, P. O. G., Prytherch, J., Salisbury, D. J., et al. (2015a). Warm-air advection, air mass transformation and fog causes rapid ice melt. *Geophysical Research Letters*, *42*(13), 5594–5602. https://doi.org/10.1002/2015GL064373

Tjernström, M., Shupe, M. D., Brooks, I. M., Persson, P. O. G., Prytherch, J., Salisbury, D. J., et al. (2015b). Warm-air advection, air mass transformation and fog causes rapid ice melt. *Geophysical Research Letters*, *42*(13), 5594–5602. https://doi.org/10.1002/2015GL064373

Tyrlis, E., Bader, J., Manzini, E., & Matei, D. (2021). Reconciling different methods of high-latitude blocking detection. *Quarterly Journal of the Royal Meteorological Society*, *147*(735), 1070–1096. https://doi.org/10.1002/qj.3960

Tyrlis, E., Bader, J., Manzini, E., Ukita, J., Nakamura, H., & Matei, D. (2020). On the role of ural blocking in driving the warm Arctic—Cold Siberia pattern. *Quarterly Journal of the Royal Meteorological Society*, *146*(730), 2138–2153. https://doi.org/10.1002/qj.3784

Tyrlis, E., Manzini, E., Bader, J., Ukita, J., Nakamura, H., & Matei, D. (2019). Ural blocking driving extreme Arctic sea ce loss, cold Eurasia, and stratospheric vortex weakening in autumn and early winter 2016–2017. *Journal of Geophysical Research: Atmospheres*, *124*(21), 11313–11329. https://doi.org/10.1029/2019JD031085

Tyrlis, E., Tymvios, F. S., Giannakopoulos, C., & Lelieveld, J. (2015). The role of blocking in the summer 2014 collapse of Etesians over the Eastern Mediterranean. *Journal of Geophysical Research*, *120*(14), 6777–6792. https://doi.org/10.1002/2015JD023543

Wernli, H., & Papritz, L. (2018). Role of polar anticyclones and mid-latitude cyclones for Arctic summertime sea ice melting. *Nature Geoscience*, *11*(2), 108–113. https://doi.org/10.1038/s41561-017-0041-0

Woods, C., & Caballero, R. (2016). The role of moist intrusions in winter Arctic warming and sea ice decline. *Journal of Climate*, *29*(12), 4473–4485. https://doi.org/10.1175/JCLI-D-15-0773.1

Yao, Y., Luo, D., Dai, A., & Simmonds, I. (2017). Increased quasi stationarity and persistence of winter ural blocking and Eurasian extreme cold events in response to Arctic warming. Part I: Insights from observational analyses. *Journal of Climate*, *30*(10), 3549–3568. https://doi.org/10.1175/JCLI-D-16-0261.1

You, C., Tjernström, M., & Devasthale, A. (2020). Warm-air advection over melting sea-ice: A Lagrangian case study. *Boundary-Layer Meteorology*, *179*, 99–116. https://doi.org/10.1007/s10546-020-00590-1

You, C., Tjernström, M., & Devasthale, A. (2021a). Eulerian and Lagrangian views of warm and moist air intrusions into summer Arctic. *Atmospheric Research*, *256*, 105586. https://doi.org/10.1016/j.atmosres.2021.105586

You, C., Tjernström, M., & Devasthale, A. (2021b). On warm and moist air intrusions into winter Arctic. *Atmospheric Chemistry and Physics Discussions*, *2021*(3), 1–29. https://doi.org/10.5194/acp-2021-610